

Claudin-7 (CLDN7) is overexpressed in gastric cancer and promotes gastric cancer cell proliferation, invasion and maintains mesenchymal state

Z. WU[‡], J. SHI[‡], Y. SONG, J. ZHAO, J. SUN, X. CHEN, P. GAO, Z. WANG^{*}

Department of Surgical Oncology and General Surgery, The First Affiliated Hospital of China Medical University, 155 North Nanjing Street, Heping District, Shenyang City 110001, PR China

**Correspondence: josieon826@sina.cn*

‡Contributed equally to this work.

Received May 21, 2017 / Accepted July 22, 2017

Gastric cancer (GC) ranks as the fourth most common cancer worldwide and is among the most aggressive types of cancer. Claudin-7 (CLDN7) has been found to be aberrantly expressed in some types of cancers. However, the expression and role of CLDN7 in gastric cancer (GC) remain largely unknown. In this study, we have performed the largest expression analysis study to date of CLDN7 in 113 pairs of human GC tissues and non-tumorous adjacent tissues. We found CLDN7 expression is significantly elevated in GC tissues, and the overexpression of CLDN7 is closely related to lymph node metastasis. Furthermore, we observed that CLDN7 executes an oncogenic function, promoting cancer cell proliferation, invasion, and epithelial–mesenchymal transition in GC. Given this oncogenic role of CLDN7 in GC formation and progression, CLDN7 may have an indispensable potential for future anti-metastatic and therapeutic applications.

Key words: Gastric cancer, CLDN7, metastasis, Epithelial-mesenchymal transition

Gastric cancer (GC) ranks as the fourth most common cancer worldwide and is among the most aggressive types of cancer, with approximately 70,000 deaths annually [1]. Cancer cells often exhibit the capacity to detach from their original position, safely pass through the circulatory system, and eventually survive in distant sites, growing to form a metastatic tumor [2]. Metastasis is regarded as the main cause of cancer-related mortality in GC [3]. While many investigations have studied the underlying mechanisms of GC metastasis, the potential roles of tight junction proteins in metastasis are scarcely covered.

Tight junctions are located at the most apical position of epithelial cellular connections and contribute to the formation of cell-to-cell adhesions [4, 5]. Claudin, a critical component of tight junctions, contains four transmembrane domains and two extracellular loops which can bind claudin proteins to adjacent cells or other molecules, implying that they may participate in inter- or intracellular signaling pathways [6, 7]. Claudin-7 (CLDN7), an important member of the claudin family, has been well documented for its pivotal role in constituting tight junctions and maintaining cell-to-cell adhesions [8, 9]. In recent years, CLDN7 has been found to be aberrantly expressed in various types of cancers [10–15], especially those derived from epithelial cells, indicating

that CLDN7 may play role in cancer initiation and progression. For example, the expression of CLDN7 was found to be elevated in ovarian cancer [11] and hepatocellular cancer [14] tissues compared to normal tissues. Moreover, some researchers found that CLDN7 may perform an oncogenic function through promoting invasion and epithelial–mesenchymal transition (EMT) in ovarian cancer and colon cancer [11, 16]. However, the role of CLDN7 in GC progression and metastasis still remains largely unstudied.

Until now, the expression profile of CLDN7 was only confined to GC tissues and normal tissues in mice [17]; the expression pattern of CLDN7 in human GC tissues was lacking. Based on the large quantity of GC patient samples regularly processed by our institution, we were equipped to study the expression of CLDN7 in human GC tissues compared to their NATs and explore the effect of CLDN7 on GC cell proliferation, invasion, and epithelial–mesenchymal transition (EMT) through a series of experimental assays.

Materials and methods

Ethics statement and human tissue samples. This research was supported by the Research Ethics Committee of China Medical University. Informed consent was obtained

from all patients enrolled in this study. All 113 pairs of human GC tissue samples and their matched non-tumorous adjacent tissues were obtained from GC patients who accepted surgical resection at the First Hospital of China Medical University between 2007 and 2010. All included 113 patients were pathologically diagnosed with GC by two experienced pathologists. The patients hadn't received any preoperative chemotherapy or radiotherapy before surgical resection. One part of each sample was cut and specially stained by hematoxylin-eosin (H&E) for histopathological analysis. The histological grade of the GC tissues was assessed corresponding to the seventh TNM staging of the International Union against Cancer (UICC)/American Joint Committee on Cancer (AJCC) system.

Cell culture. Human GC cell line SGC-7901 was purchased from the Institute of Biochemistry and Cell Biology at the Chinese Academy of Sciences (Shanghai, China). AGS cells were obtained from ATCC (Manassas, VA). The RPMI 1640 medium (Hyclone, GE, USA) containing 10% fetal bovine serum was used to culture the SGC-7901 and AGS cells. The cells were cultured at 37°C in a humidified incubator (Thermo, Waltham, MA, USA) which provided an environment containing 5% carbon dioxide.

RNA extraction and real-time PCR. Total RNA extraction and real-time PCR was performed as described in our previous study [18]. The reverse transcription of RNA was performed using the PrimeScript RT Reagent Kit (Takara) corresponding to the manufacturer's instructions. The quantitative real-time PCR was performed in a system containing diluted cDNA template, SYBR green II (Takara), diluted forward and reverse primers (10 µM), and RNase-free water. The volume of each component was referred to the protocol from a previous study. Primers used are listed in Table S1.

Protein extraction and western blot. Total protein extraction was performed using a Total Protein Extraction Kit (KeyGen) according to the manufacturer's instructions. The proteins were separated by SDS-polyacrylamide gel electrophoresis (SDS-PAGE) and then transferred from gel onto PVDF membranes (Millipore). Antibodies used were as follow: E-cadherin (Santa Cruz, CA, USA, sc-8426), Twist1 (Abcam, Shanghai, China, ab50518), MMP-9 (Wanleibio, Shenyang, China, WL01580), and β-tubulin (Sigma-Aldrich, St. Louis, MO, USA, T7816). After incubation with peroxidase-conjugated affinipure goat anti-mouse IgG or peroxidase-conjugated affinipure goat anti-rabbit IgG, the blots were detected using the GelCapture version software (DNR Bio-Imaging Systems, Jerusalem, Israel). β-tubulin was used as a loading control for western blots.

Immunofluorescence analysis. Different cells were cultured and fixed in a 24-well plate and incubated with antibodies specific for E-cadherin (1:200, Abcam, ab76055) and MMP9 (1:200, Abcam, ab119906). After incubating with secondary antibodies, the nuclei were stained by adding DAPI (1:1000, Invitrogen, D3571). Finally, the cells were observed via Leica DMI3000 B (Leica).

Transfection. In order to construct eukaryotic expression vectors, CLDN7 cDNA was synthesized and cloned into a pEX-2 (Gene Pharma) plasmid. Meanwhile, an empty vector was also constructed as a negative control named pEX2-NC. DNA sequencing experiment was applied to validate the nucleotide sequences. For knockdown experiments, the siRNA (RIBOBIO, Guangzhou, China) for CLDN7 were synthesized. The GC cells were seeded onto a six-well plate and the plasmids or siRNA were transfected into cells through Lipofectamine 2000 reagent (Invitrogen) for 6 hours. Six hours later, the medium was replaced with fresh medium, and then the cells were incubated for 48 hours till they could be used for functional experiments. The efficiency of transfection was evaluated by real-time PCR.

Cell counting kit 8 assay. Cell proliferation was evaluated through a cell counting kit 8 (CCK-8, Dojindo). Forty-eight hours after transfection, cells were re-suspended and counted. Approximately 2.5×10^3 cells were placed into 96-well culture plates and incubated for 1, 2, 3 and 4 days. In each well of the plates 10 µL CCK-8 was added and then incubated at 37°C for 1 hour. The optical density (OD) value was determined by a microplate reader (Bio-Rad, California, USA) at a wavelength of 450 nm.

Transwell invasion assay. Transwell invasion assays were performed by applying the transwell (Corning, NY, USA) and matrigel (BD Biosciences, San Jose, CA, USA) corresponding to the manufacturer's protocol. Cells were trypsinized and re-suspended in serum-free medium. Then, the cells (approximately 5×10^4) were added into the upper compartment of the chamber. After incubating at 37°C with 5% CO₂ for twenty-four hours, the chamber membrane was cut down and affixed to glass slides. Ten pictures of the slides were randomly taken using a Leica DMI300B microscope (Leica, Wetzlar, Germany). Then, these ten pictures were used to count the number of cells passing through the matrigel.

Fluorescence-activated cell sorting (FACS). Cells were digested by trypsin without EDTA and re-suspended to generate single-cell suspensions. Before cell-cycle analysis, the cells were fixed overnight at 4°C in 70% cold ethanol, stained with propidium iodide in a cell cycle detection kit (KeyGen Biotech, Nanjing, China) corresponding to the manufacturer's protocol, and analyzed using the FACS calibur flow cytometer (BD Biosciences) and BD Cell Quest software. For assessing cell apoptosis, cells were stained with Annexin V-APC and propidium iodide (Annexin V-APC Apoptosis Detection Kit, KeyGEN) according to the manufacturer's instructions. All samples were detected by the LSRFortessa (BD Bioscience).

Colony formation assay. The 0.6% and 0.3% agarose was prepared with RPMI medium containing 10% FBS. The 0.6% agarose with RPMI medium containing 10% FBS was firstly plated on the bottom of six-well plate. After the 0.6% agarose became solidified, the cells suspended in 0.3% agarose with RPMI medium containing 10% FBS were added onto the top of the 0.6% agarose prepared with the same medium.

The plates were incubated in a 37°C incubator containing 5% CO₂. After four weeks, the cell colonies were fixed for 15 minutes using methanol and then stained with Giemsa for 15 minutes. Then, the colonies were observed using a Leica DMI300B microscope (Leica, Wetzlar, Germany).

Animal experiments. 2×10⁶ cells in 0.2 ml RPMI medium containing 10% FBS were subcutaneously injected into the right armpit region of five-week-old female BALB/c nude mice. The nude mice were randomly divided into two groups (n=6 for each group). The tumor size was measured every three days with calipers. Twenty-one days after injection, the mice were sacrificed. The subcutaneous tumors were then isolated, and the size and weight of tumor lump were measured. For all animal experiments, the operators and investigators were blinded to the group allocation. All experimental procedures involving animals were done in accordance with the institutional ethical guidelines for animal experiments.

Statistical analysis. RNA expression levels in GC tissues relative to control tissues were calculated via the formula $2^{-\Delta\Delta CT}$, with $\Delta\Delta CT$ representing the difference in ΔCT values between the GC tissues and paired non-tumorous adjacent tissues ($\Delta\Delta CT = \Delta CT_{GC \text{ tissues}} - \Delta CT_{non-tumorous \text{ adjacent tissues}}$). ΔCT signifies the difference in CT value between the target and endogenous reference (GAPDH; $\Delta CT = CT_{CLDN7 \text{ mRNA}} - CT_{GAPDH}$). For all experiments, data are described by using the mean \pm 1 standard deviation (SD). At least 3 separate experiment results were used to calculate the mean value. Meanwhile, we apply the SPSS 19.0 computer software (SPSS Inc., Chicago, IL, USA) to carry out statistical analysis including Student's t test and nonparametric tests. For nonparametric tests, when comparing 2 groups, we choose the Mann-Whitney U test. We use Kruskal-Wallis test for comparing the difference among three or more groups. The Kaplan-Meier method with log-rank test was used for survival analysis. In this study, $p < 0.05$ was regarded as statistically significant.

Results

CLDN7 is upregulated in GC tissues and correlates with lymph node metastasis. In order to define CLDN7 expression profiles in GC, we evaluated the expression of CLDN7 mRNA from 113 pairs of GC tissues and non-tumorous adjacent tissues through real-time PCR. We found that CLDN7 is upregulated in GC tissues compared with the matched non-tumorous adjacent tissues ($p < 0.05$). ΔCT values for CLDN7 in cancer tissues and non-tumorous adjacent tissues were 5.47 ± 3.00 and 5.83 ± 3.41 , respectively (Figure 1A). Among the 113 patients, 68 patients (60.17%) presented higher expression of CLDN7 in GC tissues compared with non-tumorous adjacent tissues and the remaining 45 patients (38.82%) showed lower expression of CLDN7 (Figure 1B).

We evaluated the relationship between CLDN7 mRNA expression and clinic-pathological characteristics in GC

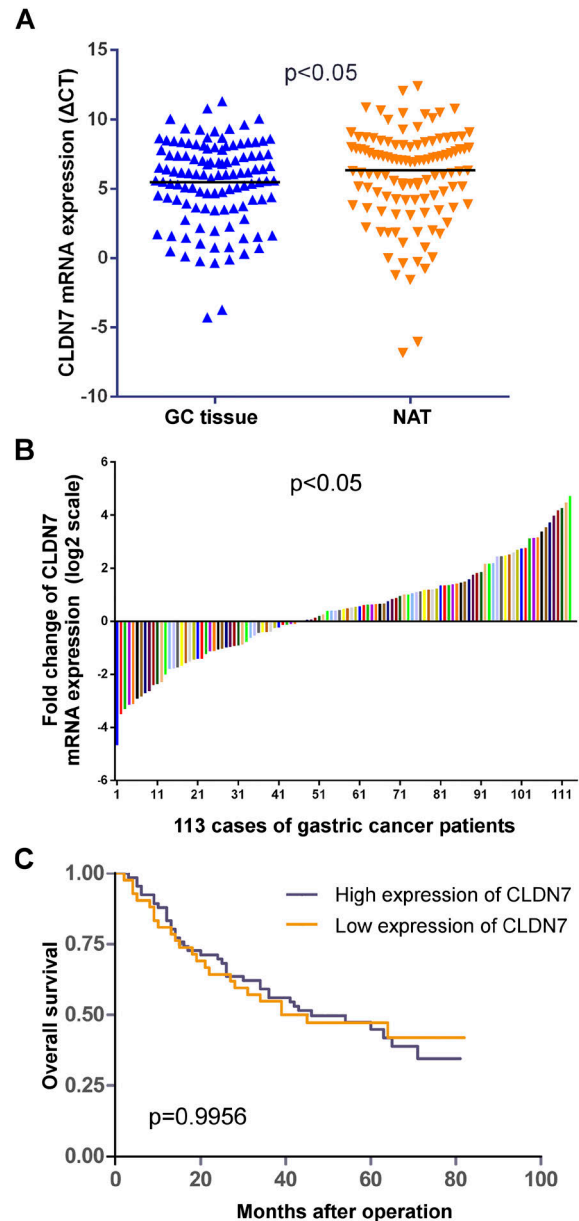


Figure 1. Expression of CLDN7 in human GC tissues and paired non-tumorous adjacent tissues. (A) ΔCT of CLDN7 in GC tissues and non-tumorous adjacent tissues. GAPDH was used as a reference. $\Delta CT = CT_{CLDN7} - CT_{GAPDH}$. Data are presented as mean \pm SD. All experiments were independently conducted three times to obtain the presented data. (B) Expression levels of CLDN7 in 113 gastric cancer patients. Expression of CLDN7 was quantified by real-time RT-PCR. Data are presented as log base 2 of the fold change in GC tissues relative to non-tumorous adjacent tissues. In each case, experiments were conducted in triplicate and repeated three times. (C) Kaplan-Meier analysis of the relationship between CLDN7 expression and overall survival.

patients. We found that higher expression of CLDN7 is significantly correlated with lymph nodes metastasis (Table 1) and patients with lymphatic metastasis exhibit higher CLDN7 expression than those free of lymph node metastasis. Intriguingly, we found that male patients and patients of

Table 1. Comparison of expression levels of CLDN7 mRNA with clinicopathological characteristics in patients with gastric cancer.

Clinicopathological characteristics	Number	Relative expression of CLDN7 mRNA ^a	p-value
Gender			0.024*
male	86	1.08 (0.45–2.60)	
female	27	2.27 (1.31–3.34)	
Age(years)			0.015*
≤61	56	1.73 (0.87–3.45)	
>61	57	0.94 (0.36–2.41)	
Tumor size			0.777
≤5	62	1.32 (0.48–2.69)	
>5	51	1.47 (0.59–2.82)	
Histological grade			0.889
well differentiated	38	1.46 (0.70–2.34)	
poor differentiated	75	1.31 (0.49–2.98)	
Lauren grade			0.244
intestinal type	43	1.56 (0.74–3.53)	
diffuse type	70	1.12 (0.48–2.53)	
pT stage			0.196
T1+T2	24	1.09 (0.30–2.92)	
T3+T4	89	1.45 (0.57–2.63)	
TNM stage			0.55
I-II	38	0.90 (0.27–1.88)	
III	75	1.57 (0.70–4.53)	
Metastatic lymph nodes			0.043*
Positive	85	1.48 (0.57–3.25)	
Negative	28	1.06 (0.17–2.24)	
Invasion into lymphatic vessels			0.241
Positive	38	1.42 (0.62–4.74)	
Negative	75	1.31 (0.46–2.60)	
Invasion into venous system			0.133
Positive	1	0.15	
Negative	112	1.39 (0.52–2.72)	

^aMedian relative expression (25th–75th percentile).

*Indicated statistical significance (p<0.05).

younger age tended to present higher expression levels of CLDN7. There was no significant statistical difference between high CLDN7 expression and other clinic-pathological parameters such as patients' tumor size, histological grade, Lauren grade, macroscopic grade, growth method, invasion depth, lymphatic vessel invasion, or venous invasion (Table 1). Meanwhile, Kaplan-Meier analysis showed there was no significant relationship between CLDN7 expression levels and overall survival (Figure 1C).

CLDN7 overexpression promotes cell proliferation, invasive capacity and maintains mesenchymal state *in vitro*. In order to assess the effect of CLDN7 on cell proliferation, we first constructed CLDN7 overexpressing GC cells and corresponding negative control (NC) cells in SGC-7901 and AGS cell lines. We verified the expression of CLDN7 in the CLDN7 overexpressing cells via real-time PCR, and the expression level of CLDN7 was obviously higher than in the NC cells (Supplementary Figure 1A–1B). Subsequently,

CCK8 was performed to determine the effect CLDN7 had on cell proliferation. The results showed that CLDN7 overexpression increased the proliferative capacity of GC cells compared with parallel NC cells in both SGC-7901 and AGS cell lines. In order to investigate the effect of CLDN7 on GC cell invasion, transwell assay was performed and the results showed that CLDN7 overexpressing SGC-7901 and AGS cells both have higher invasion capacity than control cells (Figure 2A–2D).

In an attempt to gain insight into the mechanism of how CLDN7 might promote GC cell proliferation, cell cycle distribution and apoptosis of CLDN7 overexpressing cells was detected using fluorescence-activated cell sorting (FACS). There was no significant statistical difference in either cell cycle distribution or cell apoptosis between CLDN7 overexpressing cells and NC cells (Figure 2E–2F).

Given that CLDN7 could significantly enhance the invasive capacity of GC cells, as shown by our transwell result, and promote EMT as determined by a study in colorectal cancer [16], we next evaluated the expression of invasion-related markers and EMT markers at both the transcriptional and translational levels. Analysis of invasion-related markers, mesenchymal markers, and epithelial markers via real-time PCR revealed that overexpression of CLDN7 enhanced expression of MMP9 and Twist and reduced E-cadherin expression at the transcriptional level (Figure 3A). Western blot and immunofluorescence analysis results supported the observations, showing that overexpression of CLDN7 could also enhance expression of MMP9 and reduce E-cadherin expression at the translational level (Figure 3B–3C).

CLDN7 knockdown inhibits cell proliferation, invasion and EMT *in vitro*. To further support the above results, we knocked down CLDN7 in SGC-7901 and AGS cell lines through siRNA (Supplementary Figure 1C–1D). The results of CCK-8 assay showed that CLDN7 knockdown cells (si-CLDN7 cells) possessed slower proliferation rate than the control cells (si-NC cells) in both SGC-7901 and AGS cell lines. Meanwhile, si-CLDN7 cells showed attenuated invasive capacity compared with the si-NC cells (Figure 4A–4D). Subsequently, we detected the expression of EMT markers and invasion-related markers in si-CLDN7 and si-NC cells via real-time PCR and western blot. The results of real-time PCR showed that CLDN7 knockdown increased expression of E-cadherin and led to reduced expression of MMP9 (Figure 4E). Western blot result showed increased expression of E-cadherin and decreased expression of MMP9 (Figure 4F).

CLDN7 overexpression promotes colony formation and *in vivo* tumor growth. Colony formation assay was performed to further validate the effect of CLDN7 on GC cells proliferation. We found that CLDN7 overexpression significantly enhanced the colony formation capacity of GC cells compared with the control cells (Figure 5A). Subsequently, we performed xenograft assay by subcutaneously injecting CLDN7 overexpressing cells and control

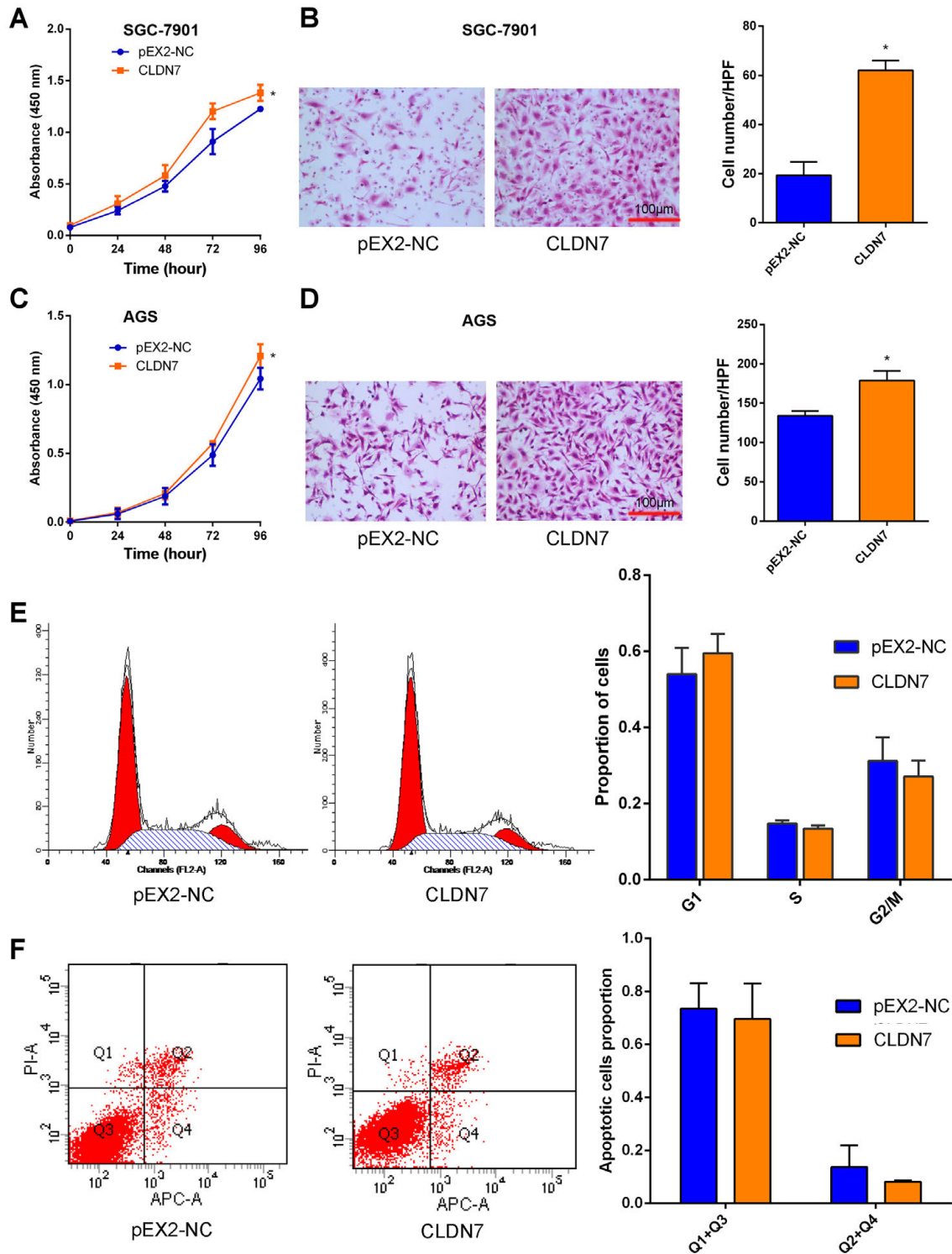


Figure 2. CLDN7 overexpression promotes cell proliferation, invasive capacity and maintains mesenchymal state *in vitro*. (A) Cell proliferation was assessed daily for 4 days using the CCK-8 assay in CLDN7 knockdown SGC-7901 cells. (B) Transwell assay was used to evaluate the invasion in CLDN7 knockdown SGC-7901 cells. Cells were incubated for 24h and then counted under the microscope. (C) Cell proliferation was assessed daily for 4 days using the CCK-8 assay in CLDN7 knockdown AGS cells. (D) Transwell assay was used to evaluate the invasion in CLDN7 knockdown AGS cells. Cells were incubated for 24 h and then counted under the microscope. (E) FACS analysis showed no significant changes in the G1, S and G2/M phases between CLDN7 overexpressing cells and NC cells. (F) Cells were stained with both Annexin V-APC and PI. Cells positive for Annexin V-APC were counted as apoptotic cells. The data are presented as the proportion of apoptotic cells. For (B) and (D), original magnification×200, scale bars = 100µm. Data are presented as mean ± SD. *means p<0.05, **means p<0.01.

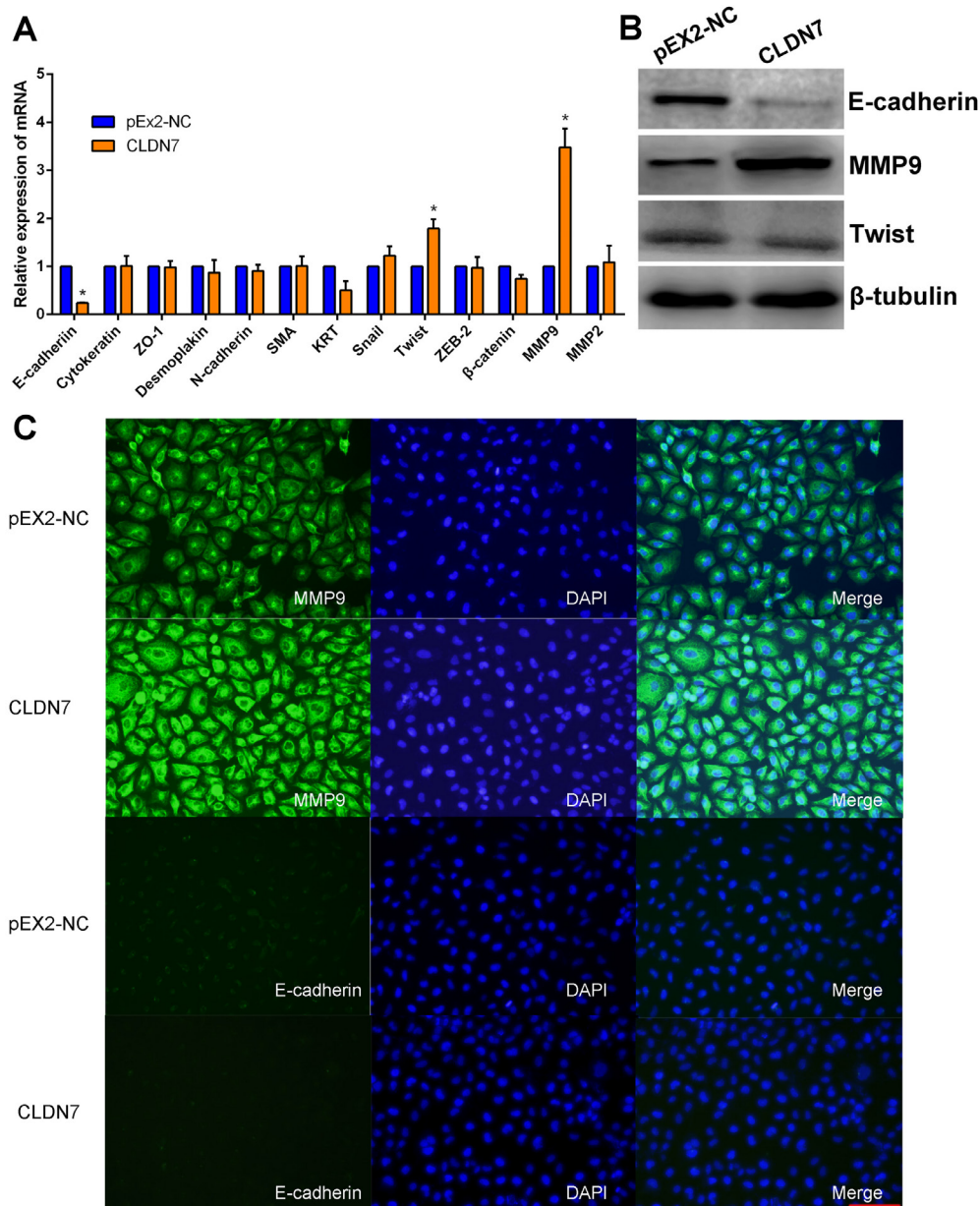


Figure 3. CLDN7 overexpression maintains mesenchymal state in GC cells. (A) The transcriptional levels of EMT related markers detected by real-time PCR. (B) The translational levels of EMT related markers detected by western blotting. (C) The translational levels of EMT related markers detected by immunofluorescence analysis. Data are presented as mean \pm SD. * means $p < 0.05$, ** means $p < 0.01$.

cells into nude mice. Xenograft tumors grown from CLDN7 overexpressing cells displayed larger volumes and formed more rapidly than tumors grown from control cells (Figure 5B–5C). The tumors were then isolated from mice and weighed. We found the mean weight of tumors from CLDN7 group (0.261 ± 0.112) significantly larger than the control group (0.165 ± 0.082) (Figure 5C–5D). These results showed that CLDN7 overexpression can promote GC cell proliferation both *in vitro* and *in vivo*.

Discussion

CLDN7 has been well characterized for its essential functions in the formation of tight junctions and maintenance of paracellular permeability in epithelial cells [8, 9]. In recent years, altered expression of CLDN7 has been observed in various types of cancers [10–14, 19]. To the best of our knowledge, our study is the first to assess the CLDN7 expression profile in a large scale study of human GC tissue samples,

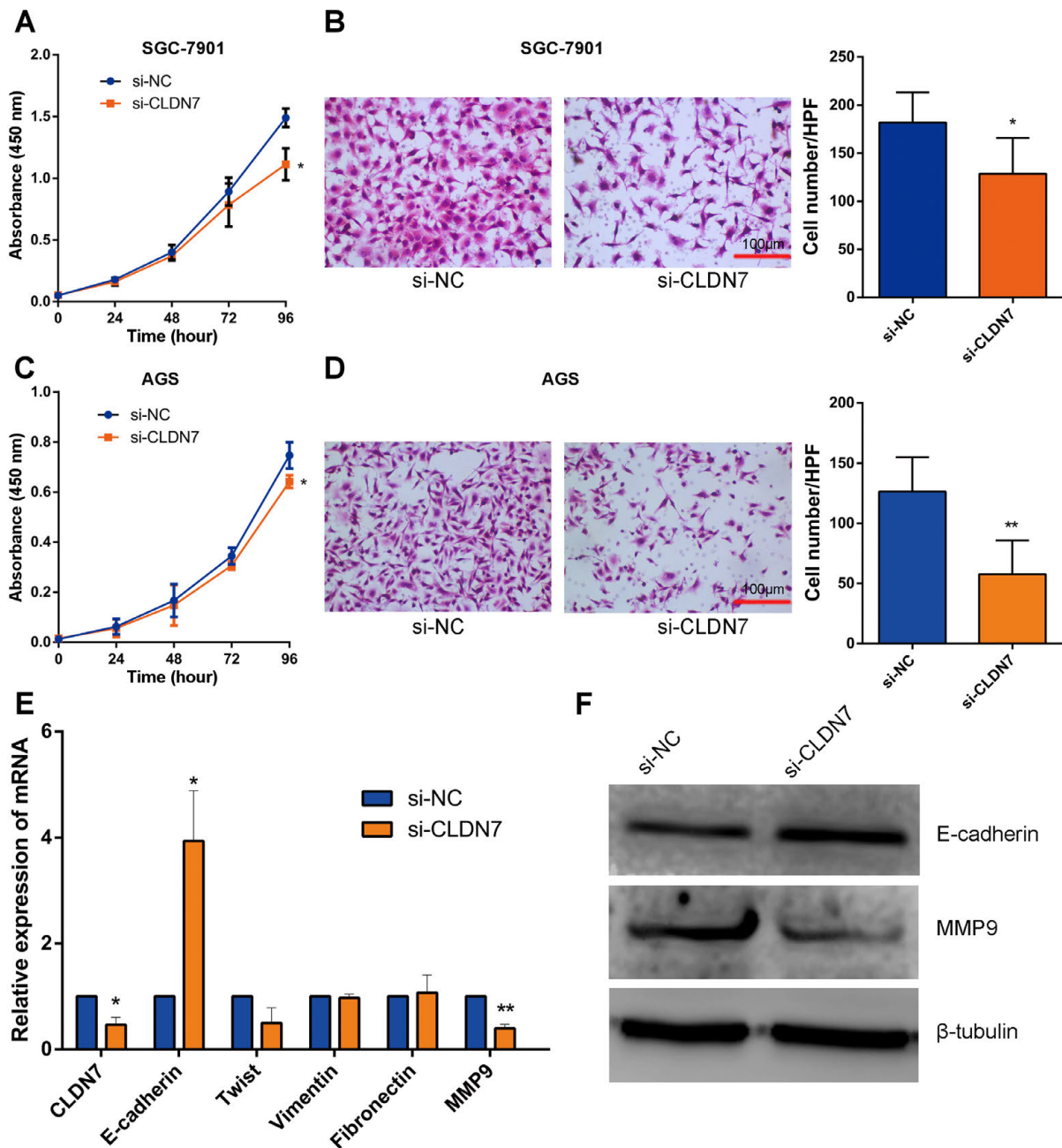


Figure 4. CLDN7 knockdown inhibits cell proliferation, invasion and EMT *in vitro*. (A) Cell proliferation was assessed daily for 4 days using the CCK-8 assay in CLDN7 knockdown SGC-7901 cells. (B) Transwell assay was used to evaluate the invasion in CLDN7 knockdown SGC-7901 cells. Cells were incubated for 24 h and then counted under the microscope. (C) Cell proliferation was assessed daily for 4 days using the CCK-8 assay in CLDN7 knockdown AGS cells. (D) Transwell assay was used to evaluate the invasion in CLDN7 knockdown AGS cells. Cells were incubated for 24 h and then counted under the microscope. (E) The transcriptional levels of EMT related markers detected by real-time PCR. (F) The translational levels of EMT related markers detected by western blot. For (B) and (D), original magnification $\times 200$, scale bars = 100 μm . Data are presented as mean \pm SD. *means $p < 0.05$, **means $p < 0.01$.

and our real-time PCR results from 113 paired human tissue samples revealed that CLDN7 was significantly overexpressed in GC tissues compared to non-tumorous adjacent tissues. This expands on a previous study reporting that CLDN7 is upregulated in mice GC tissues [17]. Consistent with the

above findings, it was also reported that CLDN7 is significantly upregulated in hepatocellular carcinoma specimens compared to non-tumor liver tissues [14]. Diverse studies have been carried out exploring the regulatory mechanisms of aberrant CLDN7 expression [20, 21]. One recent study

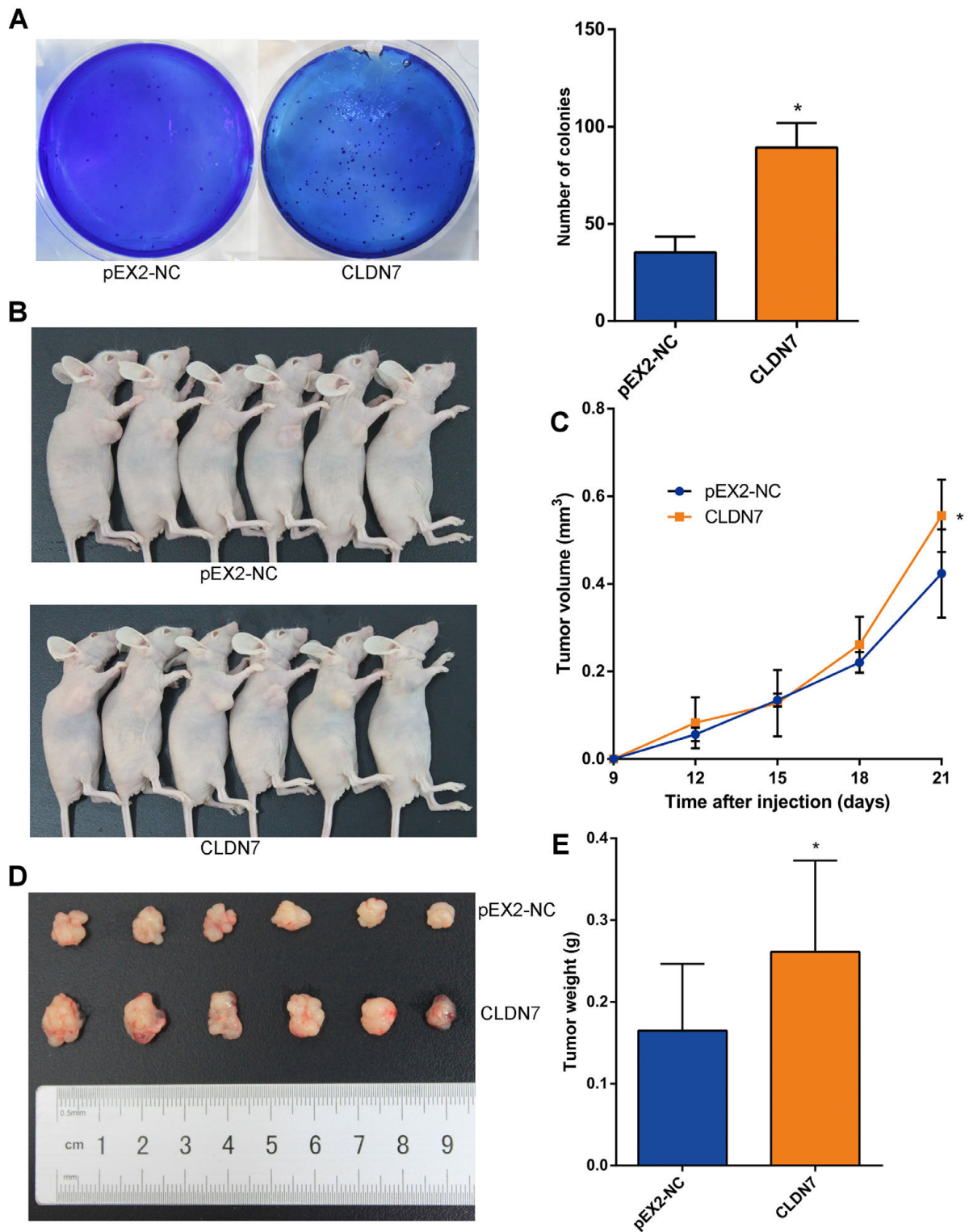


Figure 5. CLDN7 overexpression promotes colony formation and *in vivo* tumor growth. (A) Representative images of colony formation by CLDN7 overexpressing cells and control cells. The column figure left shows the colony formation number in each group. Data are presented as mean \pm SD of the tumor volumes, * means $p < 0.05$. (B) Representative images of *in vivo* tumor lumps of nude mice. Mice were sacrificed on 21st day after injection and each tumor lump was removed from the body. (C) The tumor growth curves of *in vivo* tumor volumes. Data are presented as mean \pm SD of the tumor volumes, $n=6$, * means $p < 0.05$. (D) Images of the tumors lumps of each group at the endpoint of the experiment. (E) The mean weight of tumor lumps in each group. Data are presented as mean \pm SD, $n=6$, * means $p < 0.05$.

showed that hepatocyte nuclear factor 4 α (HNF4 α) can bind the promoter region of the CLDN7 gene, thus regulating expression of CLDN7 [21]. Moreover, Nakayama et al. found that an altered status of promoter methylation may result in aberrant CLDN7 expression in colorectal carcinoma [20]. However, the exact mechanism of the altered expression of CLDN7 in GC still warrants further investigation.

We also analyzed the relationship between CLDN7 expression and clinic-pathological parameters of the enrolled patient cohort. Our results indicate that CLDN7 expression is significantly associated with lymph node metastasis, as patients with lymph node metastasis tended to have higher CLDN7 expression than those without. It is well confirmed that lymph node metastasis is an independent prognostic factor associated with the overall survival of GC patients [22–24]. This suggests that CLDN7 expression levels may function as a prognostic predicting factor for patients with GC.

Until now, it has remained controversial whether CLDN7 performs an oncogenic role or functions as a cancer suppressor. In our study, we found that CLDN7 was significantly upregulated in GC tissues compared to paired non-tumorous adjacent tissues, indicating that CLDN7 may play an oncogenic role in gastric cancer formation and progression. Therefore, we performed functional experiments to examine the function of CLDN7 *in vitro*. Our results indicate that CLDN7 can significantly promote GC cell proliferation, validating an oncogenic role for CLDN7 in GC. In accordance with our finding, a previous study [25] revealed that CLDN7 could interact with EpCAM to form a CLDN7-EpCAM complex, thus promoting tumorigenicity and tumor proliferation. One study [26] demonstrated that CLDN7 overexpression promoted gastric cancer cell proliferation through enhancing β -catenin/Tcf-4 activity. In addition, studies [27, 28] demonstrated that other claudin family members could enhance cell proliferation through regulating cell anoikis or functioning as an androgen receptor downstream molecule. Therefore, we believe that CLDN7 may influence proliferation via other pathways and more studies are needed to further investigate the mechanism of how CLDN7 enhances gastric cancer proliferation. Meanwhile, our results also found that CLDN7 can significantly enhance GC cell invasion. In consistent with our results, one study focusing on ovarian cancer suggested that CLDN7 is also found to be frequently overexpressed in ovarian cancer and is functionally involved in ovarian carcinoma invasion [11].

Epithelial-mesenchymal transition (EMT) is an essential developmental program that is often activated during tumor invasion and metastasis [29–32]. Upon detachment from the primary carcinoma, numerous types of cancer cells appear to depend on the EMT program to facilitate the majority of the steps throughout the invasion-metastasis cascade [29, 32]. Our result found that CLDN7 can promote GC cell transition from an epithelial phenotype to a mesenchymal phenotype. Through detection of EMT-related molecular markers, we

found that E-cadherin, a robust epithelial marker, was significantly decreased at both the transcriptional and translational levels. Consistent with our findings, role of CLDN7 on maintaining mesenchymal state is also supported in another study which showed that CLDN7 contributes to the shift towards EMT in colon cancer via recruiting EpCAM [16]. Additionally, we also found that the invasion-related marker matrix metalloproteinase (MMP9) was sharply elevated in CLDN7 overexpressing cells. This indicates that CLDN7 may enhance the invasive capacity of GC cells through interacting with MMP family members and increasing their activity. This is also supported by a previous study which revealed that claudin family members can promote cancer cell invasion through activating the MMP family members [33–36].

Taken together, we have performed the largest expression analysis study to date of CLDN7 in 113 pairs of human GC tissues and non-tumorous adjacent tissues. We found CLDN7 expression is significantly elevated in GC tissues, and the overexpression of CLDN7 is closely related to lymph node metastasis. Furthermore, we observed that CLDN7 executes an oncogenic function, promoting cancer cell proliferation, invasion, and maintaining mesenchymal state in GC. Given this oncogenic role of CLDN7 in GC formation and progression, CLDN7 may have an indispensable potential for future anti-metastatic and therapeutic applications.

Supplementary information is available in the online version of the paper.

Acknowledgements: We thank the department of Surgical Oncology of First Hospital of China Medical University for providing human gastric tissue samples. We also acknowledge Joseph from the Washington University School of Medicine for help in the manuscript revising. This work was supported by National Science Foundation of China (81372549), the Key Laboratory Programme of Education Department of Liaoning Province (LZ2015076) and Scientific Programme of Science & Technology Department of Liaoning Province (2015225002).

References

- [1] TORRE LA, BRAY F, SIEGEL RL, FERLAY J, LORTET-TIEULENT J et al. Global cancer statistics, 2012. *CA Cancer J Clin* 2015; 65: 87–108. <https://doi.org/10.3322/caac.21262>
- [2] FIDLER IJ. The pathogenesis of cancer metastasis: the ‘seed and soil’ hypothesis revisited. *Nat Rev Cancer* 2003; 3: 453–458. <https://doi.org/10.1038/nrc1098>
- [3] SHAH MA. Update on metastatic gastric and esophageal cancers. *J Clin Oncol* 2015; 33: 1760–1769. <https://doi.org/10.1200/JCO.2014.60.1799>
- [4] STEED E, BALDA MS, MATTER K. Dynamics and functions of tight junctions. *Trends Cell Biol* 2010; 20: 142–149. <https://doi.org/10.1016/j.tcb.2009.12.002>
- [5] SCHNEEBERGER EE, LYNCH RD. The tight junction: a multifunctional complex. *Am J Physiol Cell Physiol* 2004; 286: C1213–1228. <https://doi.org/10.1152/ajpcell.00558.2003>

- [6] LAL-NAG M, MORIN PJ. The claudins. *Genome Biol* 2009; 10: 235. <https://doi.org/10.1186/gb-2009-10-8-235>
- [7] VAN ITALLIE CM, ANDERSON JM. Claudins and epithelial paracellular transport. *Annu Rev Physiol* 2006; 68: 403–429. <https://doi.org/10.1146/annurev.physiol.68.040104.131404>
- [8] LADWEIN M, PAPE UF, SCHMIDT DS, SCHNOLZER M, FIEDLER S et al. The cell-cell adhesion molecule EpCAM interacts directly with the tight junction protein claudin-7. *Exp Cell Res* 2005; 309: 345–357. <https://doi.org/10.1016/j.yexcr.2005.06.013>
- [9] KOHNO Y, OKAMOTO T, ISHIBE T, NAGAYAMA S, SHIMA Y et al. Expression of claudin7 is tightly associated with epithelial structures in synovial sarcomas and regulated by an Ets family transcription factor, ELF3. *J Biol Chem* 2006; 281: 38941–38950. <https://doi.org/10.1074/jbc.M608389200>
- [10] KOMINSKY SL, ARGANI P, KORZ D, EVRON E, RAMAN V et al. Loss of the tight junction protein claudin-7 correlates with histological grade in both ductal carcinoma in situ and invasive ductal carcinoma of the breast. *Oncogene* 2003; 22: 2021–2033. <https://doi.org/10.1038/sj.onc.1206199>
- [11] DAHIYA N, BECKER KG, WOOD WH, 3RD, ZHANG Y, MORIN PJ. Claudin-7 is frequently overexpressed in ovarian cancer and promotes invasion. *PLoS One* 2011; 6: e22119. <https://doi.org/10.1371/journal.pone.0022119>
- [12] ALIKANOGU AS, GUNDUZ S, DEMIRPENCE O, SUREN D, GUNDUZ UR et al. Expression pattern and prognostic significance of claudin 1, 4 and 7 in pancreatic cancer. *Asian Pac J Cancer Prev* 2015; 16: 4387–4392.
- [13] SUREN D, YILDIRIM M, KAYA V, ELAL R, SELCUK OT et al. Expression patterns of claudins 1, 4, and 7 and their prognostic significance in nasopharyngeal carcinoma. *J BUON* 2015; 20: 212–217.
- [14] HOLCZBAUER A, GYONGYOSI B, LOTZ G, TORZSOK P, KAPOS-NOVAK P et al. Increased expression of claudin-1 and claudin-7 in liver cirrhosis and hepatocellular carcinoma. *Pathol Oncol Res* 2014; 20: 493–502. <https://doi.org/10.1007/s12253-013-9683-4>
- [15] BROKALAKI EI, WEBER F, SOTIROPOULOS GC, DAOU-DAKI M, CICINNATI VR et al. Claudin-7 expression in hepatocellular carcinoma. *Transplant Proc* 2012; 44: 2737–2740. <https://doi.org/10.1016/j.transproceed.2012.09.009>
- [16] PHILIP R, HEILER S, MU W, BUCHLER MW, ZOLLER M et al. Claudin-7 promotes the epithelial-mesenchymal transition in human colorectal cancer. *Oncotarget* 2015; 6: 2046–2063. <https://doi.org/10.18632/oncotarget.2858>
- [17] JOHNSON AH, FRIERSON HF, ZAIKA A, POWELL SM, ROCHE J et al. Expression of tight-junction protein claudin-7 is an early event in gastric tumorigenesis. *Am J Pathol* 2005; 167: 577–584. [https://doi.org/10.1016/S0002-9440\(10\)62999-9](https://doi.org/10.1016/S0002-9440(10)62999-9)
- [18] ZHAO JH, SUN JX, SONG YX, CHEN XW, YANG YC et al. A novel long noncoding RNA-LOWEG is low expressed in gastric cancer and acts as a tumor suppressor by inhibiting cell invasion. *J Cancer Res Clin Oncol* 2016; 142: 601–609. <https://doi.org/10.1007/s00432-015-2071-6>
- [19] YAMADA G, MURATA M, TAKASAWA A, NOJIMA M, MORI Y, SAWADA N, et al. Increased expressions of claudin 4 and 7 in atypical adenomatous hyperplasia and adenocarcinoma of the lung. *Med Mol Morphol* 2016; 49: 163–169. <https://doi.org/10.1007/s00795-016-0135-6>
- [20] NAKAYAMA F, SEMBA S, USAMI Y, CHIBA H, SAWADA N et al. Hypermethylation-modulated downregulation of claudin-7 expression promotes the progression of colorectal carcinoma. *Pathobiology* 2008; 75: 177–185. <https://doi.org/10.1159/000124978>
- [21] FARKAS AE, HILGARTH RS, CAPALDO CT, GERNER-SMIDT C, POWELL DR et al. HNF4alpha regulates claudin-7 protein expression during intestinal epithelial differentiation. *Am J Pathol* 2015; 185: 2206–2218. <https://doi.org/10.1016/j.ajpath.2015.04.023>
- [22] XU YY, HUANG BJ, SUN Z, LU C, LIU YP. Risk factors for lymph node metastasis and evaluation of reasonable surgery for early gastric cancer. *World J Gastroenterol* 2007; 13: 5133–5138.
- [23] SUN Z, LI DM, WANG ZN, HUANG BJ, XU Y et al. Prognostic significance of microscopic positive margins for gastric cancer patients with potentially curative resection. *Ann Surg Oncol* 2009; 16: 3028–3037. <https://doi.org/10.1245/s10434-009-0624-0>
- [24] JIANG CG, WANG ZN, SUN Z, LIU FN, YU M et al. Clinicopathologic characteristics and prognosis of gastric cancer invading the subserosa. *J Surg Oncol* 2010; 102: 737–741. <https://doi.org/10.1002/jso.21678>
- [25] NUBEL T, PREOBRASCHENSKI J, TUNCAY H, WEISS T, KUHN S et al. Claudin-7 regulates EpCAM-mediated functions in tumor progression. *Mol Cancer Res* 2009; 7: 285–299. <https://doi.org/10.1158/1541-7786.MCR-08-0200>
- [26] DARIDO C, BUCHERT M, PANNEQUIN J, BASTIDE P, ZALZALI H et al. Defective claudin-7 regulation by Tcf-4 and Sox-9 disrupts the polarity and increases the tumorigenicity of colorectal cancer cells. *Cancer Res* 2008; 68: 4258–4268. <https://doi.org/10.1158/0008-5472.CAN-07-5805>
- [27] ASHIKARI D, TAKAYAMA K, OBINATA D, TAKAHASHI S, INOUE S. CLDN8, an androgen-regulated gene, promotes prostate cancer cell proliferation and migration. *Cancer Sci* 2017; 108: 1386–1393. <https://doi.org/10.1111/cas.13269>
- [28] HUANG J, ZHANG L, HE C, QU Y, LI J et al. Claudin-1 enhances tumor proliferation and metastasis by regulating cell anoikis in gastric cancer. *Oncotarget* 2015; 6: 1652–1665. <https://doi.org/10.18632/oncotarget.2936>
- [29] MANI SA, GUO W, LIAO MJ, EATON EN, AYYANAN A et al. The epithelial-mesenchymal transition generates cells with properties of stem cells. *Cell* 2008; 133: 704–715. <https://doi.org/10.1016/j.cell.2008.03.027>
- [30] ACLOQUE H, ADAMS MS, FISHWICK K, BRONNER-FRASER M, NIETO MA. Epithelial-mesenchymal transitions: the importance of changing cell state in development and disease. *J Clin Invest* 2009; 119: 1438–1449. <https://doi.org/10.1172/JCI38019>
- [31] KALLURI R. EMT: when epithelial cells decide to become mesenchymal-like cells. *J Clinical Invest* 2009; 119: 1417–1419. <https://doi.org/10.1172/JCI39675>

- [32] THIERY JP, ACLOQUE H, HUANG RY, NIETO MA. Epithelial-mesenchymal transitions in development and disease. *Cell* 2009; 139: 871–890. <https://doi.org/10.1016/j.cell.2009.11.007>
- [33] OKU N, SASABE E, UETA E, YAMAMOTO T, OSAKI T. Tight junction protein claudin-1 enhances the invasive activity of oral squamous cell carcinoma cells by promoting cleavage of laminin-5 gamma2 chain via matrix metalloproteinase (MMP)-2 and membrane-type MMP-1. *Cancer Res* 2006; 66: 5251–5257. <https://doi.org/10.1158/0008-5472.CAN-05-4478>
- [34] AGARWAL R, D'SOUZA T, MORIN PJ. Claudin-3 and claudin-4 expression in ovarian epithelial cells enhances invasion and is associated with increased matrix metalloproteinase-2 activity. *Cancer Res* 2005; 65: 7378–7385. <https://doi.org/10.1158/0008-5472.CAN-05-1036>
- [35] IP YC, CHEUNG ST, LEE YT, HO JC, FAN ST. Inhibition of hepatocellular carcinoma invasion by suppression of claudin-10 in HLE cells. *Mol Cancer Ther* 2007; 6: 2858–2867. <https://doi.org/10.1158/1535-7163.MCT-07-0453>
- [36] LEOTLELA PD, WADE MS, DURAY PH, RHODE MJ, BROWN HF et al. Claudin-1 overexpression in melanoma is regulated by PKC and contributes to melanoma cell motility. *Oncogene* 2007; 26: 3846–3856. <https://doi.org/10.1038/sj.onc.1210155>